Supplementary Information:

NC10 bacteria in marine oxygen minimum zones

Contributors:

Cory C. Padilla[1]*, Laura A. Bristow[2]*, Neha Sarode[1], Emilio Garcia-Robledo[3], Eddy Gómez Ramírez[4], Catherine R. Benson[5], Annie Bourbonnais[6], Mark A. Altabet[6], Peter R. Girguis[7], Bo Thamdrup[2], Frank J. Stewart[1]

Affiliations and footnotes:

[1] School of Biology, Georgia Institute of Technology, Ford ES&T Building, Rm 1242, 311 Ferst Drive, Atlanta, GA 30332
[2] Department of Biology and Nordic Center for Earth Evolution (NordCEE), University of Southern Denmark, Odense, Denmark
[3] Department of Bioscience, Aarhus University, Aarhus, Denmark
[4] Centro de Investigacion en Ciencias del Mar y Limnologia (CIMAR), Universidad de Costa Rica, San Pedro de Montes de Oca, 2060
[5] Department of Molecular Biology and Biochemistry, Middlebury College, Middlebury, VT 05753
[6] School for Marine Science and Technology, University of Massachusetts Dartmouth, 706 Rodney French Blvd, New Bedford, MA 02744-1221
[7] Department of Organismic and Evolutionary Biology, Harvard University, Biological Laboratories, 16 Divinity Avenue, Cambridge, MA 02138

** These authors contributed equally to this work.*

Summary

This document contains a description of all methods used in this study, sequence accession number information, supporting text and discussion, and supplementary tables and figures.

MATERIALS AND METHODS:

Sample collection

Samples were collected from four stations (6,8,10,11) in the ETNP OMZ during the Oxygen Minimum Zone Microbial Biogeochemistry Expedition 2 (OMZoMBiE2) cruise (*R/V New Horizon*; cruise NH1410; May 10-June 8, 2014; Supplementary Figure S1) and at station #1 in the coastal OMZ of Golfo Dulce (GD) in late January 2015. The molecular and biochemical analyses performed for each sample are listed in Supplementary Table S1. Molecular data (metatranscriptome and 16S rRNA amplicon sequences) from samples collected at ETNP stations 6 and 10 in June 2013 are also included in this study; subsets of the 2013 datasets have been published in a prior study (Ganesh et al., 2015). In the ETNP, seawater from discrete depths spanning the oxic zone, lower oxycline, upper OMZ, and OMZ core was collected using Niskin bottles on a rosette or a pump profiling system (PPS; upper 400m only) alongside a Conductivity-Temperature-Depth profiler (Sea-Bird SBE 911plus or Sea-Bird 25 on the PPS) equipped with a Seapoint fluorometer and SBE43 dissolved oxygen sensor. In the GD, samples were collected from discrete depths using a hand-deployed Niskin bottle and dissolved oxygen profiles were measured with a Clark type O_2 electrode (Revsbech, 1989) mounted on a CTD (Sea & Sun Technology). Nutrient, methane, and molecular data presented throughout represent single water collections per depth.

Microbial biomass was collected for RNA analysis by sequential in-line filtration of seawater (~2-4 L) through a glass fiber disc pre-filter (GF/A, 47 mm, 1.6 μm pore-size, Whatman) and a primary collection filter (Sterivex™, 0.22 μm pore-size, Millipore) using a peristaltic pump. Sterivex filters were filled with RNA stabilizing buffer (25 mM Sodium Citrate, 10 mM EDTA, 5.3M Ammonium sulfate, pH 5.2), flash-frozen in liquid nitrogen, and stored at -80°C. Less than 20 min elapsed between sample collection (water on deck) and fixation in buffer. Replicate Sterivex filters for DNA analysis were collected from equivalent water volumes following RNA collection, but were instead filled with lysis buffer (50 mM Tris-HCl, 40 mM EDTA, 0.73 M Sucrose) before freezing.

Oxygen concentrations

In addition to the CTD-mounted SBE43 sensor used in the ETNP and Clark type O_2 electrode used in the GD, a high-resolution Switchable Trace amount OXygen (STOX) sensor was used to measure oxygen concentration at nanomolar levels within both the ETNP and GD OMZs. The STOX sensor was connected to an *in situ* unit (Unisense A/S) and the data acquisition was performed as described by Revsbech et al. (2011). The calibration of the STOX was done using paired values of the SBE sensor or Clark type O_2 electrode and STOX at relatively high oxygen concentrations for the STOX sensor but lower than the maximum values for the *in situ* STOX unit. Changes in sensitivity due to temperature changes were compensated for as described by Tiano et al. (2014b). Oxygen concentrations were analyzed during the upcasts, when both SBE and STOX sensors are more stable and the release of oxygen from polymers in the instruments should be minimized.

Nitrite concentrations

Samples for measuring nitrite concentration were collected in acid-washed HDPE bottles and either analyzed within 6 hours of collection (GD) or frozen until analysis (ETNP). Concentrations were determined spectrophotometrically using the Griess method, with a Westco SmartChem 200 (Unity Scientific) or Turner Trilogy (Turner Designs).

Methane quantification

Sample preparation: 20 ml (50 ml in the GD) borosilicate glass crimp top vials (Supelco) were flushed with at least three volumes of sample water. Once filled, 5 ml of sample was carefully withdrawn with a syringe. Then, 2 ml of 1N HCl (or 750 µl of 6N HCl in the case of the 50 ml vials) were added as preservative, and vials were sealed with 1 cm thick blue butyl rubber stoppers and aluminum crimp caps. Blanks were collected in the same manner, except deionized water from the shipboard MilliQ system was used in lieu of seawater. Samples were collected in duplicate from each sampling depth. Post-collection, all samples were stored at room temperature.

Quantification: For quantification, all vials were heated upside down (to prevent gas from escaping the stopper) in a dry sand bath to 99°C. The headspace of each vial was then recovered using a 20 gauge needle connected via PEEK tubing to a vacuum-purged 10 ml autosampler vial (Agilent). A glass gastight syringe with a second 20 gauge needle was filled with 0.2 µm-filter-sterilized and degassed seawater, and used to displace the remaining gas from the original sample vial into the autosampler vial. The methane samples were run on an Agilent 7890A Gas Chromatograph (GC) fitted with an Agilent 25 m x 320 µm x 30 µm Molsieve 5A column (part #CP7536) and coupled to an Agilent 5975C Mass Spectrometer Detector (MSD) modified by the manufacturer for enhanced analyses of lower mass compounds. An Agilent 7697A headspace (HS) sampler was used to deliver gas from the 10 ml vials into the GC-MSD. Each sample was quantified as follows: 1) each sample vial was equilibrated in the HS to 80°C for 1.5 minutes, and then pressurized in the HS to 103 Kpa (15 psi) with ultra-high purity helium, 2) headspace gas was transferred to a 1 mL loop kept at 105°C using the default loop fill mode, 3) the sample in the loop was injected into the GC over 0.5 min through a transfer line kept at 110 °C, 4) the sample entered the GC injector kept at 100 °C in split 1:1 mode, and then was sent through the Molsieve column at a constant rate of 1 ml min^{-1}, 5) the oven was kept at 35 °C for 10 min and then ramped to 325°C at 60°C min^{-1}, 6) the sample was ionized by electron impact at 70 eV via the MSD source kept at 300 °C, and 7) the ion intensity at m/z 15 (100 ms dwelling time) and m/z 16 (500 ms dwelling time) was acquired using the Selective Ion Mode and an electron amplifier gain of 20 to enhance sensitivity. Post-run, the m/z 16 peak was integrated using Agilent Chemstation™ Software and used for quantification. Calibration curves for each run were calculated using a series of samples prepared every 2-3 days using the following method: 10 mL headspace vials were filled with 5 mL of NaCl solution (3.5 mg/L in deionized water) and crimp-capped. Pure methane or methane dilutions were added to a series of vials to prepare the calibration series. In some cases, methane dilutions were prepared volumetrically in Helium purged serum vials (Chemglass Inc). The calibration samples were allowed to equilibrate for 10 min after vigorous shaking before analysis with the GC-MSD.

RNA/DNA extraction

RNA was extracted from Sterivex filters using a modification of the *mir*Vana™ miRNA Isolation kit (Ambion). Filters were thawed on ice, and RNA stabilizing buffer was expelled via syringe from Sterivex cartridges and discarded. Cells were lysed by adding Lysis buffer and miRNA Homogenate Additive (Ambion) directly to the cartridge. Following vortexing and incubation on ice, lysates were transferred to RNAase-free tubes and processed via acid-phenol:chloroform extraction according to the kit protocol. The TURBO DNA-free™ kit (Ambion) was used to remove DNA, and the extract was purified using the RNeasy MinElute Cleanup Kit (Qiagen).

DNA was extracted from Sterivex filters using a phenol:chloroform protocol. Cells were lysed by adding lysozyme (2 mg in 40 µl of lysis buffer per filter) directly to the Sterivex cartridge, sealing the caps/ends, and incubating for 45 min at 37°C. Proteinase K (1 mg in 100 µl lysis buffer, with 100 µl 20% SDS) was added, and cartridges were resealed and incubated for 2 hours at 55°C. The lysate was removed, and DNA was extracted once with Phenol:Chloroform:Isoamyl Alcohol (25:24:1) and once with Chloroform:Isoamyl Alcohol (24:1) and then concentrated by spin dialysis using Ultra-4 (100 kDa, Amicon) centrifugal filters.

16S rRNA gene quantitative PCR

Quantitative PCR (qPCR) was used to count total bacteria and NC10-like 16S rRNA gene copies in DNA extracted from Sterivex filters. Total 16S counts were obtained using SYBR® Green-based qPCR and universal bacterial 16S primers 1055f and 1392r, as in Ganesh et al. (2015). Ten-fold serial dilutions of DNA from a plasmid carrying a single copy of the 16S rRNA gene (from *Dehalococcoides mccartyi*) were included on each qPCR plate and used to generate standard curves, with a detection limit of ~6 gene copies ml^{-1}. Assays were run on a 7500 Fast PCR System and a StepOnePlus™ Real-Time PCR System (Applied Biosystems). All samples were run in triplicate (20 µL each) and included 1X SYBR® Green Supermix (BIO-RAD), 300 nM of primers, and 2 µL of template DNA (diluted 1:100). Thermal cycling involved: incubation at 50°C for 2 min to activate uracil-N-glycosylase (UNG), followed by 95 °C for 10 min to inactivate UNG, denature template DNA, and activate the polymerase, followed by 40 cycles of denaturation at 95°C (15 sec) and annealing at 60°C (1 min).

Counts of NC10-like 16S rRNA genes followed the protocol of Ettwig et al. (2009). Prior, to qPCR, DNA from the OMZ core at station 6 in the ETNP was screened using primers qP1F and qP2R, designed based on known NC10 sequences from freshwater habitats and flanking an ~200 bp region of the 16S rRNA gene, under the following thermal cycler conditions: initial melting for 3 min at 94°C, followed by 25 cycles of denaturation at 92°C for 1 min, annealing at 55 °C for 1.5 min, and elongation at 72°C for 1.5 min, with a final elongation step at 72°C for 10 min. Amplicons of the expected product size were detected via gel electrophoresis, purified, and cloned using the TOPO TA cloning kit (Life Technologies) according to manufacturer instructions. Sanger sequencing of a subset of clones revealed consistent sequences with top BLASTN matches to environmental NC10 clones in the GenBank database (Supplementary Table S3). DNA from these clones was used as template for generating standard curves for qPCR screens of all samples. NC10-specific 16S rRNA gene counts were obtained using SYBR® Green-based qPCR and primers qP1F and qP2R, as in Ettwig et al. (2009). Assays were run on a 7500 Fast PCR System and a StepOnePlus™ Real-

Time PCR System (Applied Biosystems). All samples were run in triplicate (20 µL each) and included 1X SYBR® Green Supermix (BIO-RAD), 300 nM of primers, and 2 µL of template DNA. Thermal cycling involved an initial denaturing step of 95°C for 3 min followed by 40 cycles of 95°C for 1 min, 63°C for 1 min, and 72°C for 1 min. After a final extension for 5 min at 72°C, melting curve analysis was carried out at temperatures from 60°C to 95°C.

pmoA PCR, cloning, sequencing, and phylogenetic analysis

The *pmoA* gene encoding subunit A of particulate methane monooxygenase has been used extensively for phylogenetic characterization of methanotrophs. To confirm the presence of and to describe the diversity of the OMZ NC10-like community, *pmoA* was PCR-amplified from a subset of samples (Supplementary Table S1), cloned and sequenced, and used for phylogenetic analysis. PmoA genes were amplified using nested PCR. The first round of PCR used the primers A189b and cmo682 targeting anaerobic methanotroph *pmoA,* and was followed by a second PCR with primers cmo182 and cmo568 (see Luesken et al. (2011) for primer sequences). Thermal cycler conditions for both rounds of amplification were: 4 min at 94°C, followed by 35 cycles of denaturation at 94°C for 1 min, annealing at 52 °C for 1 min, and elongation at 72°C for 1.5 min, with a final elongation step at 72°C for 10 min. All PCR reactions were run with 45 µL Platinum® PCR SuperMix (Life Technologies), 1 µL of 10 µM forward primer, 1 µL of 10 µM reverse primer, 1 µL DNA template, and 2 µL sterile nuclease-free water. PCR products were visualized on agarose gels to confirm the expected size range, and then purified and concentrated using the QIAquick PCR purification kit (Qiagen).

Clone libraries of *pmoA* amplicons were constructed using the TOPO TA cloning kit (Life Technologies). Purified PCR products were inserted into the pCR 2.1 TOPO Vector and transformed into One Shot TOP10 chemically competent *E. coli* cells. Cells were grown overnight at 37°C on LB plates containing 50 µg/mL ampicillin and spread with 40 µL of 50 mg/ml X-gaL. White colonies were selected and grown overnight in LB broth at 37°C. Plasmids were then extracted from cultured cells using the PureLink Quick Plasmid Miniprep Kit (Life Technologies). PCR with M13 Forward and M13 Reverse primers was used to confirm the presence and correct length of inserts. Inserts were then purified using the QIAquick PCR Purification kit and sent to the Georgia Genomics Facility for Sanger sequencing on an Applied Biosystems 3730xl DNA Analyzer using BigDye Terminator v3.1 cycle sequencing (Life Technologies).

The recovered *pmoA* nucleotide sequences were aligned (clustalW), revealing 3 unique sequence variants out of 26 total clones analyzed from the ETNP, and 1 unique phylotype out of 2 clones analyzed from the GD. Representatives of each variant were aligned using the software MEGA6 (Tamura et al., 2013) with environmental NC10-like *pmoA* sequences from Genbank, *pmoA* from the sequenced 'Ca. M. oxyfera genome, *pmoA* sequences from known aerobic methanotrophs, and Thaumarchaeota ammonia monooxygenase (*amoA*) sequences (outgroup). Aligned nucleotides were trimmed to the maximum possible length spanning all sequences, translated into amino acids in MEGA (standard genetic code), yielding a final alignment of 88 sites and 53 unique sequences – GenBank Accession numbers of database sequences are provided in Supplementary Figure S2. Aligned amino acids were used for phylogenetic reconstruction via maximum likelihood (ML) and neighbor-joining (NJ) methods using the Dayoff model bootstrapped at 1000 replicates, with uniform rates and complete deletion. Both ML and NJ methods resulted in nearly identical topologies. Only ML results are shown.

Transcriptome sequencing and analysis

Community cDNA sequencing was used to characterize microbial gene transcription in biomass (Sterivex filter fraction) from a subset of OMZ samples. From the ETNP, these included 2014 samples (n=5) from the lower oxycline (75 m) and OMZ core (300 m) at station 6, and the upper OMZ (100 m, secondary chlorophyll maximum), nitrite maximum (150 m), and OMZ core at station 10. These data were analyzed along with five station 6 datasets generated previously (Ganesh et al., 2015); 2013 datasets were collected on June 19th, 2013 and spanned the upper oxycline (30 m), lower oxycline (85 m), oxic-nitrite interface (91 m), secondary chlorophyll maximum (100 m), secondary nitrite maximum OMZ (125 m), and OMZ core (300 m) at station 6. From the GD, metatranscriptomes were generated from the Sterivex filter fraction of samples from 90, 100, and 120 m within the anoxic zone.

Community RNA was prepared for sequencing using the ScriptSeq™ v2 RNA-Seq Library preparation kit (Epicentre). cDNA was synthesized from fragmented total RNA (rRNA was not removed) using reverse transcriptase and amplified and barcoded using ScriptSeq™ Index PCR Primers (Epicenter) to generate single-indexed cDNA libraries. cDNA libraries were pooled and sequenced on an Illumina MiSeq using a 500 cycle kit. Sequence counts are listed in Supplementary Table S4.

Analysis of transcripts followed that of Ganesh et al. (2015). Barcoded sequences were de-multiplexed and low quality reads (Phred score < 25) were removed. Paired-end sequences were merged using custom scripts incorporating the FASTX toolkit (http://hannonlab.cshl.edu/fastx_toolkit/index.html) and USEARCH algorithm, with criteria of minimum 10% overlap and 95% nucleotide identity within the overlapping region. rRNA transcripts were identified with riboPicker (Schmieder et al., 2012) (and taxonomically classified using open reference picking in the software pipeline QIIME v1.8.0 (Caporaso et al., 2010) according to standard protocols. Merged non-rRNA sequences were queried via BLASTX against the NCBI-nr database (November 2013). To compare the representation of NC10-like bacteria in the metatranscriptome across samples, the NC10-transcript pool was identified using the lowest common ancestor (LCA) criteria in MEtaGenome ANalyzer 5 (MEGAN5) (Huson et al., 2011), according to the NCBI taxonomy, with counts normalized as a proportion of total protein-coding transcript sequences per sample (those with matches to NCBI-nr above bit score 50) following standardization to a uniform sequencing depth (Supplementary Table S2). In order to more fully explore the richness of NC10 transcripts (i.e., to take advantage of samples explored with greater sequencing depth), we also identified the NC10 transcript pool per sample following normalization as a proportion of total protein-coding transcript sequences (Supplementary Figure S4). Both normalization strategies yielded nearly identical relative abundance estimates (Supplementary Table S2). The LCA approach may underestimate the relative abundance of taxonomic groups with limited representation in sequence databases. The NC10 phylum is represented in nr by a single genome (*Ca*. M. oxyfera). Using the LCA approach, slowly-evolving (conserved) genes with top matches to 'M. oxyfera' may match genes of other taxa at only marginally lower bit scores and therefore potentially be classified only to "Bacteria". We therefore also present the abundances of transcripts with top BLASTX matches to genes of *Candidatus* Methylomirabilis oxyfera, with representation expressed as a percentage of the total number of sequences with BLASTX matches (>bit score 50) to NCBI-nr genes (Supplementary Table S2, S6 and Figure S3, S4). Protein-coding transcripts with top matches to known methanogen-containing archaeal lineages also were determined using MEGAN5 based on

annotations of BLASTX-identified genes.

Assembly and phylogenetic analysis of qNor transcripts:

For each metatranscriptome (n = 13), non-rRNA reads with top matches (bit score > 50) to 'M. oxyfera' via BLASTX against NCBI nr were assembled using the de novo assembler in CLC Genomics workbench 8 (http://www.clcbio.com), with a minimum contig length cutoff of 500 bp. Eight of 13 assemblies yielded contigs > 500 bp (n = 33 total). Protein-coding genes on these contigs were identified by BLASTX against NCBI nr. The search identified two full-length genes (from samples 2014 ETNP Stn10 150 m and 2013 ETNP Stn6 300 m) with matches to 'M. oxyfera' nitric oxide reductases (NOR). The corresponding amino acid sequences were aligned with NOR sequences from Ettwig et al. (2012) via Multiple Alignment using Fast Fourier Transform (MAFFT). The alignment was trimmed manually and visually inspected for substitutions in quinol binding and catalytic sites. The trimmed alignment, of 15 sequences spanning 520 aa, was used for phylogenetic analysis in MEGA6 by the Maximum Likelihood (ML) criterion. ML heuristic searches used the Le and Gascuel 2008 substitution model with a discrete Gamma distribution to model rate differences among sites and initial tree(s) obtained by Neighbor-Joining based on pairwise distances estimated using a JTT model [model selection was done using the best-fit model selection tool in MEGA6]. The tree with the highest log likelihood, along with clade bootstrap values (1000 replicates), is shown in Figure 2.

16S rRNA gene amplicon analysis

We used 16S rRNA gene amplicon sequencing of 2013 ETNP and 2015 GD samples to explore the distribution of methanogens in the OMZ (Supplementary Figure S5) (Amplicon samples from other ETNP sites were not available at the time of sequencing). *[Note: Amplicons matching NC10 bacteria were not detected in this analysis, consistent with the low abundance of NC10 16S rRNA genes determined by qPCR (Figure 1).*] ETNP data from station 6 were reported in Ganesh et al. (2015); station 10 data have not been reported previously. GD data were generated in this study. Briefly, amplicons were synthesized using Platinum® PCR SuperMix (Life Technologies) with primers F515 and R806, encompassing the V4 region of the 16S rRNA gene (Caporaso et al., 2011). These primers are used primarily for bacterial 16S rRNA genes analysis, but also amplify archaeal sequences. Both forward and reverse primers were barcoded and appended with Illumina-specific adapters. Thermal cycling involved: denaturation at 94°C (3 min), followed by 30 cycles of denaturation at 94°C (45 sec), primer annealing at 55°C (45 sec) and primer extension at 72°C (90 sec), followed by extension at 72°C for 10 min. Amplicons were analyzed by gel electrophoresis to verify size (~400 bp) and purified using RapidTip2 PCR purification tips (Diffinity Genomics). Amplicons from different samples were pooled at equimolar concentrations and sequenced on an Illumina MiSeq using a 500 cycle kit with 5% PhiX as a control.

Demultiplexed amplicon read pairs were quality trimmed with Trim Galore (Babraham Bioinformatics), using a base Phred33 score threshold of Q25 and a minimum length cutoff of 100bp. High quality paired reads were then merged using the software FLASH. These pre-processed merged reads were then analyzed using the software pipeline QIIME v1.8.0 (Caporaso et al., 2010), according to standard protocols. Briefly, reads were first screened for chimeras using QIIME's identify_chimeric_seqs.py script with Usearch61. Non-chimeric sequences were

clustered into Operational Taxonomic Units (OTUs) at 97% sequence similarity using open-reference OTU picking protocol with the script pick_open_reference_otus.py. Taxonomy was assigned to representative OTUs from each cluster using the Greengenes reference database (Aug 2013 release) in QIIME.

Rate measurements

Process rates were determined using stable isotope tracers (^{15}N, ^{13}C) added to incubations of seawater from stations 6, 8, and 10 in the ETNP and station 1 in the GD (Supplementary Table S1, S7). All incubations were run in duplicate and followed procedures to minimize oxygen contamination, as described by De Brabandere et al. (2014). Water for incubations was taken directly from Niskin bottles or the PPS and transferred to 250 ml glass bottles. Bottles were overflowed (three volume equivalents) and sealed without bubbles with deoxygenated butyl rubber stoppers and stored in the dark at *in situ* temperature. Amendments of $^{15}NO_2^-$ + $^{13}CH_4$ and $^{15}NO_2^-$ + $^{13}CH_4$ + acetylene were conducted at all depths and all stations. Each bottle was spiked with ^{15}N-labelled substrate, purged with a helium - carbon dioxide (800 ppm) mixture for approximately 20 minutes, dispensed into 12-ml exetainers (Labco, UK) using a slight overpressure, and immediately capped with deoxygenated lids. Headspaces of 2 ml helium were introduced into each exetainer and flushed twice. After headspace flushing, $^{13}CH_4$ (as gas or saturated water) and acetylene (as saturated water) additions were injected directly into each exetainer through the septum. Final concentrations were 5 μM $^{15}NO_2^-$, 1 μM $^{13}CH_4$, and 200 μM acetylene. For each treatment, duplicate exetainers were preserved with 100 μl of 50% (w/v) $ZnCl_2$ at the start of the incubation, and again at 18 and 36 hours at stations 6 and 8 and 24, 48, 96 and 240 hours at station 10 and station 1 GD.

Production of $^{14}N^{15}N$ and $^{15}N^{15}N$ was determined using a gas-chromatography isotope ratio mass spectrometer (GC-IRMS), as in Dalsgaard et al. (2012). Rates were calculated based on the slope of the linear regression of $^{14}N^{15}N$ and $^{15}N^{15}N$ with time. T-tests were applied to determine if rates were significantly different from zero ($p < 0.05$).

The production of ^{13}C-DIC from $^{13}CH_4$ additions was determined following acidification by GC-IRMS, using the method outlined in Torres et al. (2005). The detection limit of this method was 0.6 nM d^{-1}, based on two times the standard error.

Sequence data

Single gene (16S rRNA, pmoA) data have been deposited in the NCBI GenBank database under Accession numbers KP864050 - KP864054. Metatranscriptome and amplicon sequence data have been deposited in the NCBI Sequence Read Archive under BioProject ID's PRJNA277357 and PRJNA263621.

Supplementary Results and Discussion - Transcriptomics

Metatranscriptomes confirmed that NC10-like bacteria are transcriptionally active within the two study sites, the ETNP OMZ off Manzanillo, Mexico (May 2014) and the anoxic, coastal basin of Golfo Dulce (GD), Costa Rica (January 2015) (Supplementary Tables S2, S5-S6). Community RNA from 5 ETNP samples (stations 6 and 10, 2014) and 3 GD samples from upper and core anoxic zone depths was used to create cDNA libraries and shotgun sequenced using Illumina technology. These sequence sets were analyzed along with 5 datasets spanning the oxic zone and OMZ at ETNP station 6 in June 2013; the latter were generated in a prior study using the same methods (Ganesh et al., 2015) and reanalyzed here. The relative abundance of rRNA transcripts classified as NC10 varied widely and increased with decreasing oxygen, peaking at the ETNP core (300 m) and at 90 m in the GD (Supplementary Table S2), consistent with the depths of maximum NC10 16S gene counts (Figure 1). The inverse relationship with oxygen was clearest in the 2013 ETNP data, in which 'M. oxyfera' representation increased from below detection in the oxic zone (30 m) to 0.02% of total rRNA transcripts at the OMZ core (300 m). For all samples, BLASTX against the NCBI non-redundant (nr) protein database identified mRNA transcripts with top matches to the *Ca.* M. oxyfera genome (Supplementary Table S2, S6). These trends were supported when BLASTX-identified mRNA transcripts were assigned taxonomy based on a lowest common ancestor (LCA) algorithm (Supplementary Table S2, S5). However, the abundance of 'M. oxyfera'-like transcripts was lower using the LCA approach, likely due to limited representation of NC10 in the nr database, which could prevent accurate assignment of slowly evolving genes. 'M. oxyfera'-like mRNA transcripts varied widely in relative abundance and, with the exception of the 150 m sample from ETNP station 10, paralleled the distribution of NC10 rRNA transcripts, increasing with declining oxygen and peaking at ~0.1% of total mRNA transcripts in the ETNP OMZ (Supplementary Table S2). Based on top BLAST matches, queries against NCBI-nr identified 210 unique 'M. oxyfera' genes across all ETNP samples (range: 2-112 per sample), with an average amino acid identity (AAI) of 66% to matching OMZ transcripts, and 33 genes across GD samples (average AAI: 57%) (Supplementary Table S6). These AAI values fall within the genome-wide range observed for bacteria categorized in the same genus, although lower values have been observed among strains of the same species (Konstantinidis and Tiedje, 2005).

Genes with predicted roles in dissimilatory N transformations in NC10 were detected among 'M. oxyfera'-like transcripts assignable by both top match and LCA approaches (Supplementary Figure S3, S4). These included genes for reduction of nitrate to nitrite (*narGH*), nitrite to NO (*nirS*), and NO to N_2O (*norZ*). Two *norZ* genes, encoding quinol-dependent nitric-oxide reductases (qNor), were the most abundant sequences, together representing 45% of all transcripts with top matches to 'M. oxyfera' and 51% of transcripts assignable by LCA. As described in the main text, for two samples (ETNP station 6, 300 m (2013) and station 10, 150 m (2014)), assemblies of qNor transcript fragments yielded full-length gene sequences that clustered phylogenetically non-canonical qNor variants of *Ca*. M. oxyfera hypothesized to function as putative NO dismutase enzymes. [*Sequencing coverage of the NC10-like transcript pool was insufficient to enable assembly of longer contigs representing other NC10 genes*.]

The 'M. oxyfera' transcript pool from the ETNP also contained sequences suggestive of methane oxidation by n-damo, including the methane-oxidizing pMMO enzyme. However, these sequences were at low abundance (<1% of total 'M. oxyfera' reads; Supplementary Table S6) and not detectable via LCA. All detected pMMO transcripts from the ETNP matched 'M.

oxyfera' pMMO as a top BLASTX hit; pMMO transcripts matching aerobic methanotrophs were not detected. In contrast, 'M. oxyfera'-like pMMO was not detected in the GD datasets. Rather, transcripts most similar to both soluble and particulate MMO of putative aerobic methylotrophs were recovered in the upper depths of the GD (90, 100 m; data not shown), despite anoxic conditions at these depths. The pMMO enzyme is related structurally to ammonia monooxygenase and may function non-specifically to oxidize ammonia to toxic hydroxylamine, which in other methanotrophs is then detoxified by hydroxylamine oxidoreductase (HAO) (Stein and Klotz, 2011). Interestingly, transcripts matching 'M. oxyfera' HAO were highly represented in both ETNP and GD OMZs (Supplementary Figures S3, S4, Tables S5, S6), raising the possibility of ammonia oxidation by the resident NC10 population. Overall low levels of NC10-assigned transcripts involved in methane oxidation raise the question of whether the OMZ NC10 population utilizes energy substrates other than methane. Alternatively, low representation of specific transcripts may be due to misclassification, which is possible if the OMZ NC10 population is sufficiently divergent from the 'M. oxyfera' reference.

Supplementary Results and Discussion – Rate Measurements

To search for a distinct biogeochemical indication of n-damo activity, we conducted anoxic 10-day incubations of OMZ water with ^{13}C-labeled methane and ^{15}N-labeled nitrite to measure rates of anaerobic methane oxidation and N_2 production. At all analyzed depths in the ETNP (100, 150, and 300 m at station 10), methane oxidation measurements were below the detection limit (0.6 nM d^{-1}; Supplementary Table S7). Rates at two of the three analyzed depths in the GD (100, 120 m) also were below detection. Such low rates are consistent with published rates from the ETNP of typically $\leq$ 0.1 nM d^{-1} (range 7 x 10^{-5} – 1.6 nM d^{-1}; aerobic and anaerobic oxidation not discerned; Pack et al., 2015) and with the low NC10 16S rRNA gene counts observed at both GD and ETNP sites, which would correspond to rates < 0.02 nM d^{-1} assuming specific rates similar to those determined in enrichment cultures (0.09 – 0.2 fmol CH_4 per 16S rRNA gene copy per day; Ettwig et al., 2009).

In contrast, at 90 m in the GD, the depth of maximum NC10 gene abundance, methane oxidation was measured at 2.6 ± 0.7 nM d^{-1} but was inhibited under identical conditions with the addition of acetylene, an inhibitor of pMMO. Although oxygen concentration was not continuously recorded during these incubations, prior analyses indicate that oxygen content stays below 80 nM using our incubation protocol (Ganesh et al., 2015). Together, these results raise the possibility of OMZ methane consumption by pMMO-catalyzed AOM. However, the activity of pMMO-utilizing aerobic methanotrophs in this study remains unconstrained, but is suggested by the recovery of MMO transcripts from putative aerobic methylotrophs at this depth. Similar co-occurrence of NC10 and aerobic methanotrophs has been documented previously in a lake hypolimnion (Kojima et al., 2014). Although rates of aerobic methane oxidation generally decrease sharply under sub-micromolar oxygen concentrations (Gerritse and Gottschall, 1993; Ren et al., 1997; van Bodegom et al., 2001), a contribution of aerobic methanotrophy to the oxidation rates observed in the upper GD cannot be ruled out based on previous studies suggesting aerobic methane oxidation (Tavormina et al., 2010) and/or a combined use of oxygen and nitrate (Kits et al., 2015) can occur in sub-oxic environments. Given the low abundances of NC10 genes and transcripts at the GD site, it is likely that the observed methane oxidation rates reflect contributions from other methanotrophs.

Given a predicted 4:3 ratio of N_2 production to CH_4 oxidation during n-damo (Ettwig et al.,

2010), the low methane oxidation rates observed in most OMZ samples indicate a minor contribution of n-damo to N_2 production in the OMZ compared to denitrification and anammox. Contributions from denitrification and anammox peaked at 0.3 – 2 nM d^{-1} and 1 – 5 nM d^{-1}, respectively, at nearby stations 3 and 7 in the ETNP and 8 nM d^{-1} and 115 nM d^{-1} respectively, at station 1 in the GD (Supplementary Figure S1), consistent with previous measurements from these regions (Dalsgaard et al., 2003; Babbin et al., 2014; Ganesh et al., 2015), with the differences between sites reflecting the coastal and offshore locations. The conversion rates of ^{15}N-labeled nitrite to N_2 in our 10-day methane oxidation assays (0.4 to 13.8 nM d^{-1} for the ETNP, 152 to 432 nM d^{-1} for the GD; Supplementary Table S7) were broadly consistent with these ranges, although the long incubation may have caused a stimulation of activity through bottle effects (Thamdrup et al., 2006). If coupled to oxidative processes other than methane oxidation, NO dismutation could make a larger contribution to N_2 production than suggested by our estimates.

Supplementary Results and Discussion – Conclusion

Here, the detection of NC10 in both open-ocean and coastal OMZs suggests that these bacteria are widespread in low oxygen pelagic zones. Prior studies have reported sulfate-dependent ANME archaea in anoxic water columns (Jakobs et al., 2013), and this group may be the dominant AOM community in waters replete with sulfate and devoid of nitrite. While the contribution of NC10 to OMZ methane consumption, suggested by the recovery of NC10 *pmo* genes but not yet confirmed by rate measurements, remains uncertain, the unique conditions of nitrite accumulation common in anoxic OMZs may be hypothesized to enable n-damo to effectively compete for available methane. Additionally, n-damo may have a competitive advantage over ANME under the low methane concentrations of pelagic OMZs, as the affinity of pMMO for methane is generally orders of magnitude higher than that of methyl-coenzyme M reductase, the methane-activating enzyme of methanotrophic archaea (Smith et al., 1991; Nauhaus et al., 2002; Baani and Liesack, 2008; Ettwig et al., 2008).

The detection of NC10 bacteria in OMZs suggests a need for further studies to validate the potential for internal OMZ methane cycling, potentially involving coupling to denitrification. Coastal, shelf, or slope sediments may be a source of methane to OMZ waters (Sansone et al., 2001; Pack et al., 2015), but methane could potentially also be generated internally by OMZ methanogens. In support of this hypothesis, deep sequencing of 16S rRNA gene amplicons generated from 2013 ETNP (stations 6 and 10) and GD samples from this study revealed sequences matching methanogenic Euryarchaeota. These groups were undetectable at oxic depths (30 m), but increased along the transition into the OMZ to peak in relative abundance either at (ETNP) or just below (GD) the nitrite maximum (Supplementary Figure S5). Similarly, methanogen rRNA transcripts in ETNP and GD metatranscriptomes increased in relative abundance as oxygen declined, accounting for ~0.01-0.08% of all rRNA transcripts at OMZ depths. Diverse mRNA transcripts with top matches to methanogens also were identified in metatranscriptome datasets (Supplementary Figure S5), including transcripts encoding steps of the classical pathway catalyzing CO_2 reduction to methane (Reeve et al. 1997) (Supplementary Table S8), although total counts of methanogenesis enzyme transcripts were low (<0.003% of mRNA sequences). These results raise the possibility of active methanogens in OMZs and hence a potential for internal methane cycling.

N_2 production by NC10 bacteria would represent an overlooked third route of nitrogen loss in

OMZs, along with classical denitrification and anammox. The latter are unquestionably the dominant OMZ N sinks, given the low NC10 bacterial numbers indicated here by qPCR. However, if OMZ NC10 bacteria are indeed oxidizing methane, this activity, even at low rates, may substantially affect the open ocean methane inventory. In the ETNP, for example, at a methane concentration of 20 nM and NC10 16S rRNA gene abundance of 100 copies ml^{-1} as found at the inshore stations (Figure 1), and assuming specific rates of 0.09 – 0.2 fmol CH_4 per 16S rRNA gene copy per day (Ettwig et al., 2009), we estimate a turnover time for methane of 2.7 – 6.1 years. This is similar to a recently estimated water age of 3.9 ± 0.8 years for the ETNP OMZ core (DeVries et al., 2012), which indicates that NC10 bacteria may be as important as ventilation for controlling these large open-ocean methane pools. With a much shorter estimated water residence of 35 – 57 days (Ferdelman et al., 2006), the GD OMZ is a more dynamic system, which may explain the coexistence of NC10 bacteria with a large population of [putative] aerobic methanotrophs. Although the relative importance of these two populations to methane oxidation is not clear, the establishment of an NC10 population here emphasizes that n-damo could be active in other low-oxygen pelagic zones enriched in both methane and nitrogen oxides, including oil spills and seasonal hypoxic zones (deadzones). Additionally, the presence of NC10 in the OMZ raises the possibility for interactions with other metabolic pathways, including competition with anammox for nitrite, or potentially for ammonia if NC10 monooxygenases act nonspecifically. Understanding the diversity and dynamics of coupled chemical cycles in low-oxygen waters is critical, as zones of oxygen loss are predicted to increase in both area and frequency during climate change (Stramma et al., 2008).

REFERENCES:

Baani M, Liesack W. (2008). Two isozymes of particulate methane monooxygenase with different methane oxidation kinetics are found in *Methylocystis* sp. strain SC2. *P Natl Acad Sci USA* **105:** 10203-10208.

Babbin AR, Keil RG, Devol AH, Ward BB (2014). Organic matter stoichiometry, flux, and oxygen control nitrogen loss in the ocean. *Science* **344**: 406-408.

Caporaso JG, Kuczynski J, Stombaugh J, Bittinger, Bushman FD, Costello EK *et al.* (2010). QIIME allows analysis of high-throughput community sequencing data. *Nat Meth* **7**: 335-336.

Caporaso JG, Lauber CL, Walters WA, Berg-Lyons D, Lozupone CA, Turnbaugh PJ *et al*. (2011). Global patterns of 16S rRNA diversity at a depth of millions of sequences per sample. *P Natl Acad Sci USA* **108**: 4516-4522.

Dalsgaard T, Canfield DE, Petersen J, Thamdrup B, Acuña-González J. (2003). N_2 production by the anammox reaction in the anoxic water column of Golfo Dulce, Costa Rica. *Nature* **422:** 606-608.

Dalsgaard T, Thamdrup B, Farias L, Revsbech NP. (2012). Anammox and denitrification in the oxygen minimum zone of the eastern South Pacific. *Limnol Oceanogr* **57:** 1331-1346.

De Brabandere L, Canfield DE, Dalsgaard T, Freiderich GE, Revsbech NP, Ulloa O *et al*. (2014). Vertical partitioning of nitrogen-loss processes across the oxic-anoxic interface of an oceanic oxygen minimum zone. *Environ Microbiol* **16:** 3041-3054.

DeVries T, Deutsch C, Primeau F, Chang B, Devol A. (2012). Global rates of water-column denitrification derived from nitrogen gas measurements. *Nat Geosci* **5**: 547-550.

Ettwig KF, Butler MK, Le Paslier D, Pelletier E, Mangenot S, Kuypers MMM *et al*. (2010). Nitrite-driven anaerobic methane oxidation by oxygenic bacteria. *Nature* **464**: 543-548.

Ettwig KF, Shima S, va de Pas-Schoonen KT, Kahnt J, Medema MH, Op den Camp HJ *et al.* (2008). Denitrifying bacteria anaerobically oxidize methane in the absence of Archaea. *Environ Microbiol* **10:** 3164-3173.

Ettwig KF, Speth DR, Reimann J, Wu ML, Jetten MS, Keltjens JT. (2012). Bacterial oxygen production in the dark. *Front Microbiol* **3**: 273.

Ettwig KF, van Alen T, van de Pas-Schoonen KT, Jetten MSM, Strous M. (2009). Enrichment and molecular detection of denitrifying methanotrophic bacteria of the NC10 Phylum. *Appl Environ Microbiol* **75**: 3656-3662.

Ferdelman TG, Thamdrup B, Canfield DE, Glud RN, Kuever J, Lillebaek R *et al.* (2006). Biogeochemical controls on the oxygen, nitrogen and sulfur distrabutions in the water column of Golfo Dulce: an anoxic basin on the Pacific coast of Costa Rica revisited. *Rev Biol Trop* **54:** 171-191.

Ganesh S, Bristow LB, Larsen M, Sarode N, Thamdrup B, Stewart FJ. (2015). Size-fraction partitioning of community gene transcription and nitrogen metabolism in a marine oxygen minimum zone. *ISME J* **9**: 2682-2696.

Gerritse J, Gottschall JC. (1993). Two-membered mixed cultures of methanogen and aerobic bacteria in O_2-limited chemostats. *J Gen Microbiol* **139:** 1853-1860.

Huson DH, Mitra S, Ruscheweyh HJ, Weber N, Schuster SC. (2011) Integrative analysis of environmental sequences using MEGAN4. *Genome Res* **21:** 1552-1560.

Jakobs G, Rehder G, Jost G, Kisslich K, Labrenz M, Schmale O. (2013). Comparative studies of pelagic microbial methane oxidation within the redox zones of the Gotland Deep and Landsort Deep (central Baltic Sea). *Biogeosciences* **10**: 7863-7875.

Kits KD, Klotz MG, Stein LY. (2015). Methane oxidation coupled to nitrate reduction under hypoxia by the Gammaproteobacterium *Methylomonas denitrificans*, sp. nov. type strain FJG1. *Environ Microbiol* **9:** 3219-3232.

Kojima H, Tokizawa R, Kogure K, Kobayashi Y, Itoh M, Shiah F *et al.* (2014). Community structure of planktonic methane-oxidizing bacteria in a subtropical reservoir characterized by dominance of phylotype closely related to nitrite reducer. *Sci Rep* **4:** 1-7.

Konstantinidis KT, Tiedje JM. (2005). Towards a genome-based taxonomy for prokaryotes. *J Bacteriol* **187:** 6258-6264.

Luesken FA, Zhu BL, van Alen TA, Butler MK, Diaz MR, Song B. (2011). *pmoA* primers for detection of anaerobic methanotrophs. *Appl Environ Microbiol* **77:** 3877-3880.

Nauhaus K, Boetius A, Krüger M, Widdel F. (2002). In vitro demonstration of anaerobic oxidation of methane coupled to sulphate reduction in sediment from marine gas hydrate area. *Environ Microbiol* **4:** 296-305.

Pack MA, Heintz MB, Reeburgh WS, Trumbore SE, Valentine DL, Xu X *et al*. (2015). Methane oxidation in the eastern tropical North Pacific Ocean water column. *J Geophys Res Biogeosci* **120**: 1078-1092.

Reeve JN, Nolling J, Morgan RM, Smith DR. (1997). Methanogenesis: Genes, genomes, and who's on first? *J Bacteriol* **179:** 5975-5986.

Ren T, John AA, Knowles R. (1997). The response of methane consumption by pure cultures of methanotrophic bacteria to oxygen. *Can J Microbiol* **43:** 925-928.

Revsbech NP, Thamdrup B, Dalsgaard T, Canfield DE. (2011). Construction of STOX oxygen sensors and their application for determination of O_2 concentrations in oxygen minimum zones. *Meth Enzymol* **486:** 325-341.

Revsbech NP. (1989). An oxygen microsensor with a guard cathode. *Limnol Oceanogr* **34:** 474-478.

Sansone FJ, Popp BN, Gasc A, Graham AW, Rust TM. (2001). Highly elevated methane in the eastern tropical North Pacific and associated isotopically enriched fluxes to the atmosphere. *Geophys Res Lett* **28**: 4567-4570.

Schmieder R, Lim YW, Edwards R. (2012). Identification and removal of ribosomoal RNA sequences from metatranscriptomes. *Bioinformatics* **28**: 433-435.

Smith RL, Howes BL, Garabedian SP. (1991). In situ measurement of methane oxidation in groundwater by using natural-gradient tracer tests. *Appl Environ Microbiol* **57:** 1997-2004.

Stein LY, Klotz MG. (2011) Nitrifying and denitrifying pathways of methanotrophic bacteria. *Biochem Soc T* **39:** 1826-1831.

Stramma L, Johnson GC, Sprintall J, Mohrholz V. (2008). Expanding oxygen-minimum zones in the tropical oceans. *Science* **320:** 655-658.

Tamura K, Stecher G, Peterson D, Filipski A, Kumar S. (2013) MEGA: Molecular Evolutionary Genetics Analysis Version 6.0. *Mol Biol Evol* **30:** 2725-2729.

Tavormina PL, Ussler W, Joye SB, Harrison BK, Orphan VJ. (2010). Distributions of putative aerobic methanotrophs in diverse pelagic marine environments. *ISME J* **4:** 700-710.

Thamdrup B, Dalsgaard T, Jensen MM, Ulloa O, Farias L, Escribano R. (2006). Anaerobic ammonium oxidation in the oxygen-deficient waters off northern Chile. *Limnol Oceanogr* **51:** 2145-2156.

Tiano L, Garcia-Robledo E, Dalsgaard T, Devol AH, Ward BB, Ulloa O *et al*. (2014a). Oxygen distribution and aerobic respiration in the north and southeastern tropical Pacific oxygen minimum zones. *Deep-Sea Res Pt I* **94**: 173-183.

Tiano L, Garcia-Robledo E, Revsbech NP. (2014b). A new highly sensitive method to assess respiration rates kinetics of natural planktonic communities by the use of the switchable trace oxygen sensor and reduced oxygen concentrations. *PLoS ONE.* **9:** 10-1371.

Torres ME, Mix AC, Rugh WD. (2005). Precise delta C-13 analysis of dissolved inorganic carbon in natural waters using automated headspace sampling and continuous-flow mass spectrometry. *Limnol Oceanogr Meth* **3:** 349-360.

van Bodegom P, Goudriaan J, Leffelaar P. (2001). A mechanistic model on methane oxidation in a rice rhizosphere. *Biochemistry* **55:** 145-177.

Wu ML, Ettwig KF, Jetten MSM, Strous M, Keltjens JT, van Niftrik L. (2011). A new intra-aerobic metabolism in the nitrite-dependent anaerobic methane-oxidizing bacterium *Candidatus* 'Methylomirabilis oxyfera'. *Biochem Soc T* **39:** 243-248.

Wu ML, van Teeseling MCF, Willems MJR, van Donselaar Eg, Klingl A, Rachel R *et al.* (2012). Ultrastructure of the denitrifying methanotroph "*Candidatus* Methylomirabilis oxyfera," a novel polygon-shaped bacterium. *J Bacteriol* **194:** 284-291.

Supplementary Figure S1 | Sampling sites in the ETNP and GD OMZs off Mexico and Costa Rica, respectively. ETNP samples for analysis of methane concentrations and biochemical and molecular analysis of n-damo bacteria were collected at stations 6, 8, 10, and 11 in May 2014. Additional samples used for molecular analysis were collected at stations 6 and 10 in July 2013. Stations 3 and 7 are also shown (black circles), as these indicate sites of measured anammox and denitrification rates in 2014 (as described in the main text). All samples from the GD were collected at station 1 at the far northern head of Golfo Dulce.

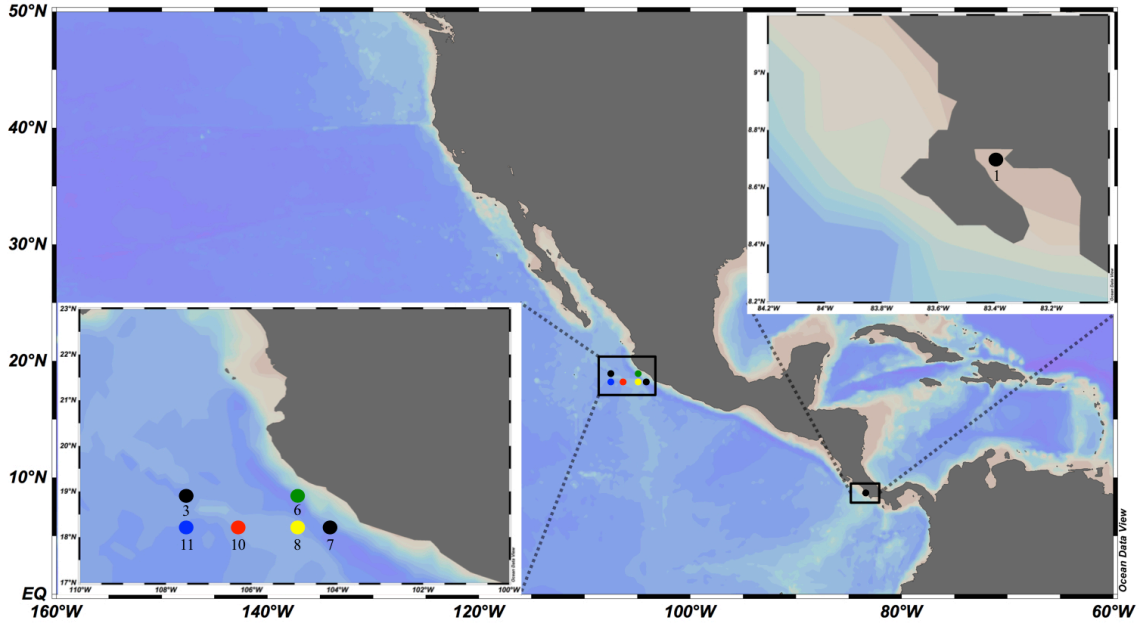

Supplementary Figure S2 | PmoA gene phylogeny. Uncollapsed version of the particulate methane monooxygenase subunit A (PmoA) gene phylogeny shown in Figure 2 (main text). PmoA sequences (n=53) recovered from the ETNP are highlighted in bold within the larger clade of NC10-like sequences from other studies, separated from PmoA of aerobic methanotrophic clades and an ammonia monooxygenase (AmoA) outgroup. Reconstruction is based on Maximum Likelihood analysis of 88 amino acids using the Dayhoff substitution model. Bootstrap values greater than 70 are shown, along with NCBI accession numbers for database sequences. The scale bar represents 50 amino-acid changes per 100 amino acids.

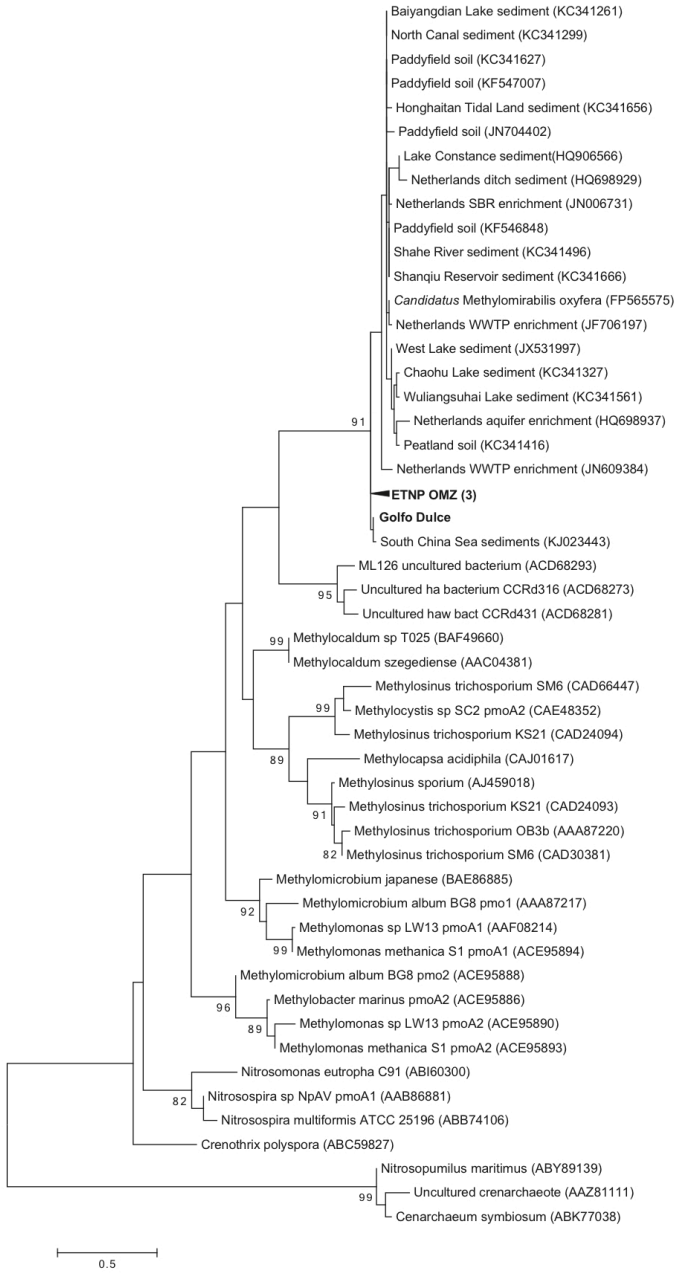

Supplementary Figure S3 | Transcription of putative n-damo genes in the ETNP (a,b) and GD (c,d) identified by LCA analysis in MEGAN5. **a,c** Abundances of transcripts assigned to Phylum NC10 using lowest common ancestor binning of BLASTX results in MEGAN5, as a % of the total number of MEGAN5-classified mRNA transcripts in each sample. **b,d** % abundances of NC10-like transcripts matching genes of the proposed pathway for denitrification-dependent AOM (diagram modified from Wu et al. (2011, 2012). Data in **c** and **d** were binned over all samples shown in **a** and **c**, respectively, with abundance colored as a percentage of the total mRNA transcripts assigned to NC10 in MEGAN. nar = nitrate reductase, nir = nitrite reductase, nor = nitric oxide reductase, mdh = methanol dehydrogenase, pmo = particulate methane monooxygenase, bc1 = cytochrome bc1 complex, ndh = NAD(P)H dehydrogenase complex, Q = coenzyme Q, hao = hydroxylamine oxidoreductase. Light gray shows potential non-specific oxidation of ammonium by pMMO, followed by detoxification of hydroxylamine to nitrite by hao. Counts reflect matches to all subunits of each enzyme.

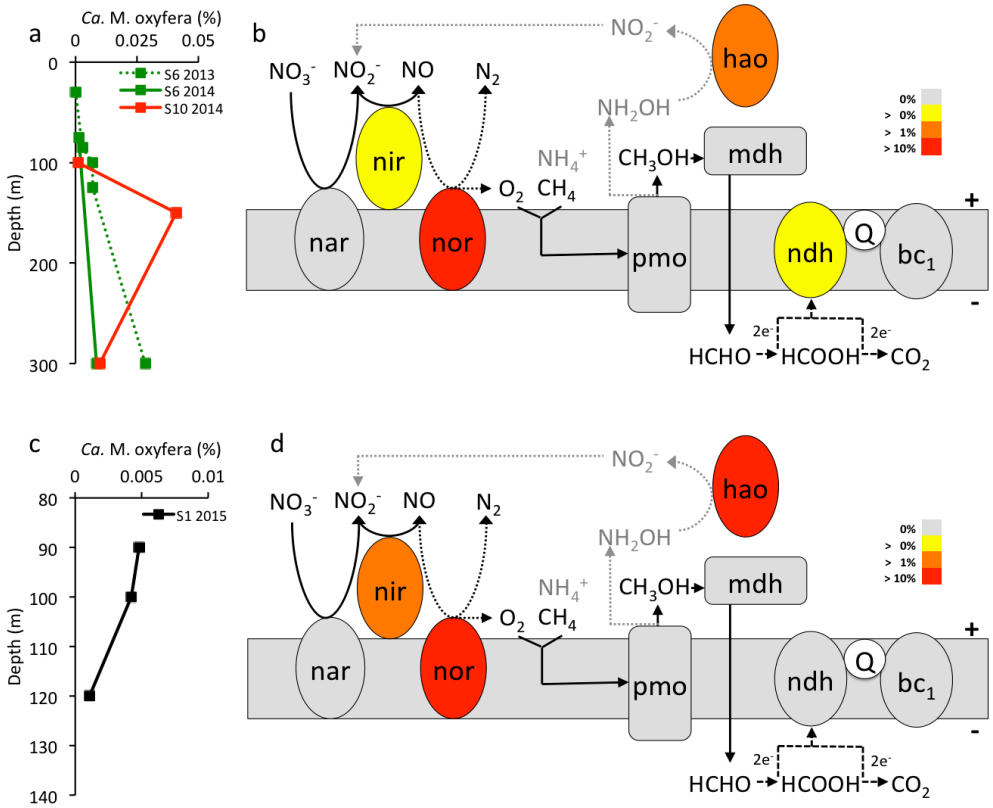

Supplementary Figure S4 | Transcription of putative n-damo genes in the ETNP (a,b) and GD OMZs identified by top BLASTX matches (c,d). **a,c** Abundances of transcripts with top matches (bit score > 50) to *Candidatus* M. oxyfera genes during BLASTX against the NCBI-nr database, as a % of the total number of mRNA transcripts in each sample. **b,d** % abundances of 'M. oxyfera'-like transcripts matching genes of the proposed pathway for denitrification-dependent AOM (diagram modified from Wu et al. (2011, 2012). Data in **b** and **d** were binned over all samples shown in **a** and **c**, respectively, with abundance colored as a percentage of the total mRNA transcripts matching 'M. oxyfera' genes. nar = nitrate reductase, nir = nitrite reductase, nor = nitric oxide reductase, mdh = methanol dehydrogenase, pmo = particulate methane monooxygenase, bc1 = cytochrome bc1 complex, ndh = NAD(P)H dehydrogenase complex, Q = coenzyme Q, hao = hydroxylamine oxidoreductase. Light gray shows potential non-specific oxidation of ammonium by pMMO, followed by detoxification of hydroxylamine to nitrite by hao. Counts reflect matches to all subunits of each enzyme.

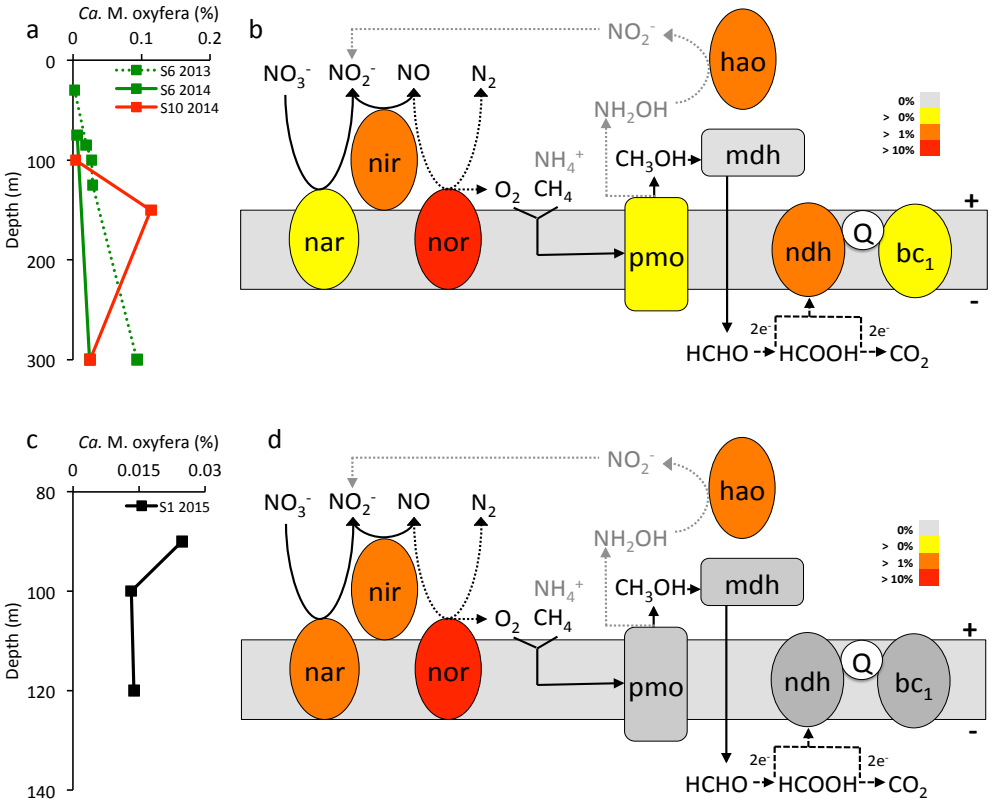

Supplementary Figure 5 | Methanogen abundance in the ETNP and GD OMZs. Percentage abundance of sequences affiliated with methanogenic Euryarchaeota in 16S rRNA gene amplicon (**left**), community rRNA transcript (**middle**), and community mRNA transcript (**right**) datasets. The vast majority (>95%) of all methanogen 16S rRNA genes affiliated with the Class Methanobacteria. The remainder matched the Class Methanomicrobia.